Available online at www.sciencedirect.com
SCIENCE DIRECT®
Geochimica et Cosmochimica Acta 70 (2006) 2856–2867
Geochimica
www.elsevier.com/locate/gca

Unusual C_{35} and C_{36} alkenones in a paleoceanographic benchmark strain of *Emiliania huxleyi*

Fredrick G. Prahl [a,*], Jean-François Rontani [b], John K. Volkman [c], Margaret A. Sparrow [a], Ida M. Royer [a]

[a] *College of Oceanic and Atmospheric Sciences, Oregon State University, Corvallis, OR 97331-5503, USA*
[b] *Laboratoire de Microbiologie de Géochimie et d'Ecologie Marines (UMR 6117), Centre d'Océanologie de Marseille, F-13288 Marseille, France*
[c] *CSIRO Marine and Atmospheric Research, GPO Box 1538, Hobart, Tasmania 7001, Australia*

Received 14 July 2005; accepted in revised form 7 March 2006

Abstract

Our specimen of the cultured *Emiliania huxleyi* strain (CCMP1742, also known as NEPCC55a) that provides the benchmark for $U^{K'}_{37}$-based paleothermometry has started producing, for reasons yet unclear, major amounts of three new alkenones identified as ω15,22-C_{35} methyl ketone, ω15,22-C_{36} ethyl ketone and ω16,23-C_{36} methyl ketone. Comparison of these structures with those established now by the same OsO_4 derivatization method applied to the di-unsaturated C_{37}, C_{38} and C_{39} alkenones typically found in this organism provides insight into the possible pathway for their biosynthesis. Isothermal batch culture experiments also show the content and composition of these new compounds change systematically and quite significantly in cells when subjected to environmental conditions such as nutrient depletion, variation in light availability and prolonged darkness. Alkenones of similarly unusual short-chain length are evident in suspended particulate materials from present day surface waters in the Ligurian Sea (Mediterranean) and in two different Holocene time horizons (Unit I and Unit II deposits) in Black Sea sediments. However, the positions of the double bonds are different from those that we now report in our culture, implying a different biosynthetic sequence. These alkenones are most likely derived from another, as yet unknown, haptophyte species. If this other organism accounts for all documented occurrences of these compounds in natural samples, then either it has a capacity for growth over a remarkably wide salinity range or surface water salinity in the early Holocene Black Sea may not have been as low as is currently believed.

1. Introduction

Alkenone unsaturation patterns as quantified by the index $U^{K'}_{37}$ (Brassell et al., 1986) provide a powerful paleoproxy for sea-surface temperature (SST) (Müller et al., 1998). Despite overall success to date with the use of this proxy, some uncertainties still exist in the alkenone-based paleothermometer (Eglinton et al., 2001 and associated articles). Possible effects due to postmortem degradation (e.g., Rontani et al., 2006a), as well as non-thermal physiological effects that alter alkenone distributions within the living algal cell (Conte et al., 1998; Epstein et al., 1998; Prahl et al., 2003) must be considered carefully. It is now clear that not all alkenone-producers synthesize identical distributions of alkenones at a given growth temperature (e.g., Volkman et al., 1995; Conte et al., 1998). Furthermore, there is increasing evidence that non-thermal effects on alkenone signatures observed in laboratory-based culture experiments are expressed to some extent in a range of natural samples including suspended particulate materials (SPM) from surface waters (Conte et al., 1995; Prahl et al., 2003, 2005), settling particulate materials captured in sediment traps (Prahl et al., 2005) and bottom sediments (Conte et al., 1995; Prahl et al., 2006). Consequently, it remains a challenge to determine the extent to which ecolog-

* Corresponding author. Fax: +1 541 737 2064.
E-mail address: fprahl@coas.oregonstate.edu (F.G. Prahl).

0016-7037/$ - see front matter © 2006 Elsevier Inc. All rights reserved.
doi:10.1016/j.gca.2006.03.009

ical and non-thermal physiological factors that shape the fossil record for $U^{K'}_{37}$ vary in their importance, both spatially and temporally, and when they would need careful consideration if accurate alkenone-based paleotemperature assessments were a primary goal.

In this paper, we document the appearance of major amounts of unprecedented C_{35} and C_{36} alkenones in a cultured strain of *Emiliania huxleyi* (CCMP1742). CCMP1742 is the same strain used to establish the original $U^{K'}_{37}$—growth temperature calibration (NEPCC55a: Prahl et al., 1988) that now serves as a benchmark for paleotemperature reconstruction purposes (Müller et al., 1998). Although there is as yet no explanation why our particular culture of this strain has started biosynthesizing these compounds, we document systematic and in many cases quite significant changes in the cellular production of these compounds that are dependent upon exposure to various non-thermal physiological stresses. These stresses, which include widely varying light intensity, nutrient depletion and prolonged, continuous darkness, are those that cells in the natural marine environment can encounter when growing within the euphotic zone or upon initial exposure to sedimentary processes that act to shape the paleorecord for these biomarkers (Prahl et al., 2006). We also report the presence of similarly unusual short-chain alkenones in SPM from the high salinity (>35) Mediterranean Sea as well as contemporary and early Holocene sediments depositing beneath much fresher (~20 or less) surface waters of the Black Sea. Chemical characterization of the compounds in these field samples shows they are not structurally identical to the new alkenones now biosynthesized by our culture of CCMP1742, implying their probable origin from some source other than *E. huxleyi*. Finally, we briefly discuss how our collective findings add to understanding of the yet largely undefined alkenone/alkenoate biosynthetic pathway in *E. huxleyi* and provide a valid reason to re-evaluate the current perception about the evolution of salinity conditions in the Black Sea during the early Holocene.

2. Materials and methods

2.1. Algal culture samples

The strain of *E. huxleyi* examined experimentally in this study was collected by others in the mid-1980s from Station PAPA in the subarctic Pacific Ocean (50°N 145°W) and deposited as '55a' in the Northeast Pacific Culture Collection (NEPCC). In 1996, a specimen of NEPCC55a was transferred to the Provasoli-Guillard National Center for Culture of Marine Phytoplankton (http://ccmp.bigelow.org), the culture collection from which we obtained it as 'CCMP1742' in early 2000. Since that time, we have maintained our stock of CCMP1742 in batch culture using 500 mL Pyrex flasks, regulated temperature (12–16 °C), cool-white fluorescent illumination (~50 μEin m^{-2} s^{-1}; daily 12 h light/dark cycle) and a standard growth medium derivative, either f/2 or f/20 both without silicate added (see recipes on the CCMP website).

During experiments, culture flasks were homogenized by gentle swirling at the same time each day and immediately sub-sampled using a sterile pipette for determination of cell density, nutrient (nitrate and *ortho*-phosphate) concentrations, and cellular alkenone content and composition. At each experimental time point, cell density was determined microscopically using a haemocytometer. Cells in known volumes of culture were also filtered using gentle vacuum onto precombusted (450 °C, 8 h), glass fiber filters (25 mm diameter, Whatman GF/F). All samples on GF/F were wrapped in aluminum foil and stored frozen (−80 °C) until needed for alkenone analysis. A volume of filtrate from each alkenone sample was also collected in an acid-cleaned, 25 mL polyethylene vial and stored frozen until needed for nutrient analysis.

2.2. Black Sea sediment samples

Two depth intervals (10–11 cm and 66–67 cm) from a Black Sea gravity core (BS4-14-2GC: 2218 m water depth, 43.078°N 34.027°E) were obtained for biomarker analysis. Since collection, the core had been stored under refrigerated conditions (~4 °C) in a sealed D-tube in the Oregon State University Core Repository. Analyzed samples were obtained from well above and below a conspicuous stratigraphic horizon in the core located at ~47 cm, demarking the interface between Unit I and Unit II deposits in the Black Sea (Arthur and Dean, 1998).

2.3. Chemical analyses

The procedure for extraction of total lipid fractions (TEL) from each GF/F filter and preparation of each TEL extract for detailed quantitative analysis of alkenone and alkenoate content and composition by capillary gas chromatography with flame ionization detection (GC-FID) is fully described elsewhere (Prahl et al., 1988, 2003). Frozen filtrate from each sampling time point was thawed and immediately analyzed for nitrate and *ortho*-phosphate concentration by routine, autoanalyzer-based, spectrophotometric methods (Strickland and Parsons, 1972).

TEL fractions were obtained from Black Sea sediments using a Dionex ASE-200 extraction system. Wet sediment samples (~2 g dry weight) were extracted (100 °C, 1500 psi) using pure methanol (3×) and then a mixture (3:1 v/v) of dichloromethane in methanol (3×). The combined extracts (~40 mL total) were subsequently chromatographed on silica gel to obtain an alkenone plus alkenoate fraction suitable for quantitative analysis by capillary GC-FID. Details of this chemical workup procedure we now employ routinely for analysis of alkenones and alkenoates in natural samples are presented elsewhere (Prahl et al., 1989).

2.4. Osmium tetroxide derivatization of biomarkers

OsO_4 (~2 mg/mg of extract) and a 1:8 pyridine–dioxane solvent mixture (5 mL) were added to each TEL fraction. The resultant solution was homogenized by swirling and then incubated at room temperature (1 h). Afterwards, a 16% (w/v) suspension of Na_2SO_3 in water–methanol (8.5:2.5, v/v) was added (6 mL) and the mixture incubated again at room temperature (1.5 h). The solution was subsequently acidified (pH 3) by dropwise addition of concentrated HCl and extracted three times with hexane–chloroform (4:1, 5 mL each). The combined extracts were dried over anhydrous Na_2SO_4, filtered and concentrated by rotary evaporation. Resultant residues were dissolved in 300 μL of a 2:1 (v/v) mixture of anhydrous pyridine and *N*,*O*-bis-(trimethylsilyl)-trifluoroacetamide (BSTFA, Supelco) and allowed to react at 50 °C for 1 h. After evaporation to dryness under a gentle stream of pre-purified nitrogen, the silylated residue was re-dissolved in a suitable volume of a 2:1 (v/v) mixture of ethyl acetate and BSTFA and analyzed by gas chromatography–mass spectrometry.

Electron impact (EI) spectra for the derivatized compounds of interest were obtained using an HP5890 Series II Plus gas chromatograph interfaced to a HP5972 benchtop quadrupole mass spectrometer (GC–MS). The GC–MS was configured with: on-column injection; a fused silica column (30 m × 0.25 mm i.d.) coated with SOLGEL-1 (0.25 μm film thickness); temperature programming (60–130 °C at 30 °C min^{-1}, from 130 °C to 300 °C at 4 °C min^{-1} followed by a 30 min hold at 300 °C); helium carrier gas (maintained at 1.04 bar throughout the temperature program and then ramped to 1.5 bar at 0.04 bar min^{-1}); 70 eV electron impact (EI) ionization with a source temperature of 170 °C and 1.5 s cycle time.

3. Results and discussion

3.1. Identification of new alkenones in cultures

For a period of almost 9 months beginning in November of 2001, our stock of CCMP1742 was maintained by routine transfers and not used for any experimental purpose. Gas chromatographic analysis of TEL fractions isolated from cells collected after this hiatus revealed a significant biochemical change had occurred for some as yet unknown reason. The cells were now biosynthesizing major amounts of three entirely new, high molecular weight compounds (Fig. 1) in addition to the commonly expected mixture of C_{37}, C_{38} and C_{39} alkenones and associated C_{36} fatty acid esters (Brassell, 1993).

The new compounds were all identified as alkenones based on interpretation of EI mass spectra obtained by capillary column GC–MS analysis (Fig. 1). The spectrum for the most abundant of the three compounds, which comprised 60–70% of the total new compounds, was consistent with a C_{35} di-unsaturated, methyl ketone (K35:2m). Spectra for the other two compounds, which occurred in almost equal relative abundance, were consistent with a C_{36} di-unsaturated, methyl (K36:2m) and ethyl (K36:2e) ketone, respectively.

TEL fractions from selected samples were subsequently treated with OsO_4 to produce di-hydroxyl derivatives of each carbon–carbon double bond in the unsaturated ketones. GC–MS analysis of the silylated, tetrahydroxy derivatives yielded EI mass spectra confirming the compound identities and allowing in each case determination of the carbon-chain position, but not the geometry of double bonds. Double bonds in K35:2m and K36:2e were located at ω15,22 positions while those in K36:2m were located at ω16,23 positions (Fig. 1). The ω15,22 finding is consistent with what is now considered structurally characteristic of the alkenone signature typifying *E. huxleyi* (Brassell, 1993 and references therein), while the ω16,23 finding was unexpected. The geometry of the double bonds in these compounds could not be determined from our results, but is assumed to be *trans* based on inference from the work of others (Rechka and Maxwell, 1988).

3.2. History of the biosynthetic change in cultures

Biosynthesis of these new alkenones by our stock of CCMP1742 was first noticed in August of 2002. At that time, the C_{35} and C_{36} compounds collectively comprised ~13% of the total C_{35}–C_{39} alkenone content (%K35,36) of isothermally grown (15 °C), exponentially dividing cells (Fig. 2A). By March of 2003, %K35,36 values measured in such cells had increased to ~32%. A year later, the same high value was observed when exponentially dividing cells were examined, indicating the ratio of new to total alkenones had stabilized.

In November of 2001, prior to the appearance of the new alkenones, $U^{K'}_{37}$ values measured in isothermally grown (15 °C), exponentially dividing cells of CCMP1742 were consistently 0.53 ± 0.024 (1σ) (Prahl and Sparrow, unpublished data). This value agreed well with that predicted by the temperature calibration equation established ~15 years earlier on another stock of the same cultured strain of *E. huxleyi* ($U^{K'}_{37} = 0.034T + 0.039$: Prahl et al., 1988). However, $U^{K'}_{37}$ values measured at an equivalent growth stage in CCMP1742 cells that were now biosynthesizing new alkenones were conspicuously lower than predicted by that equation. The difference between measured and predicted values ($\Delta U^{K'}_{37}$) increased as the ratio of new C_{35} and C_{36} compounds to total C_{35}–C_{39} alkenones (%K35,36) increased. As illustrated in Fig. 2A, when %K35,36 values reached 13% in August of 2002 and 32% in March of 2003, the calculated $\Delta U^{K'}_{37}$ values were equivalent to those expected had the original stock of CCMP1742 cells grown at ~1.3 °C and ~4.2 °C lower temperatures, respectively.

3.3. Non-thermal physiological impacts on composition in cultures

Since discovery of the new alkenones in our stock of CCMP1742, we have conducted three different types of

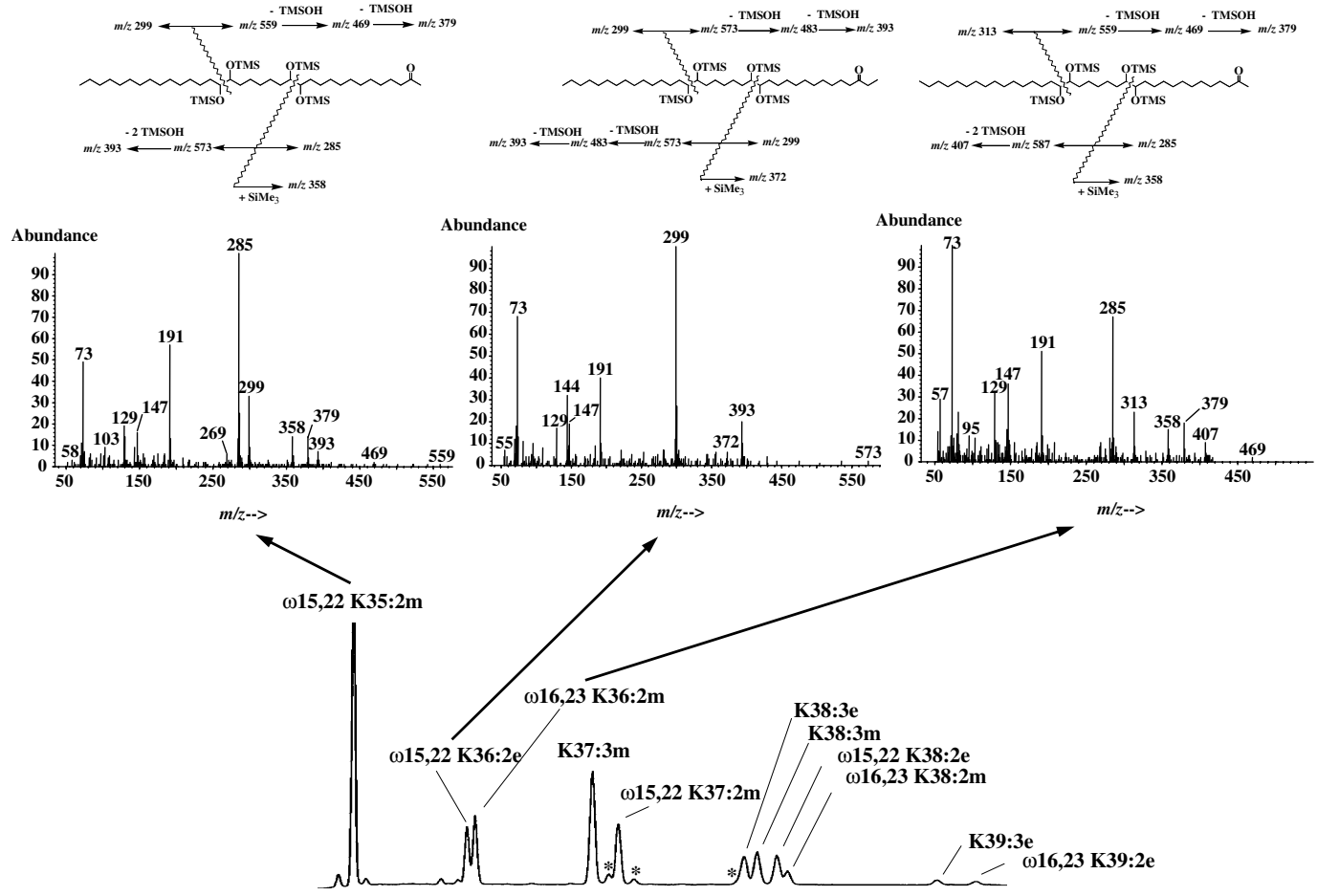

Fig. 1. Gas chromatogram illustrating the occurrence of major amounts of three new alkenones in the total extractable lipid (TEL) fractions isolated from exponentially dividing cells of *E. huxleyi* strain CCMP1742 (also referred to as NEPCC55a). Electron impact mass spectra and structural interpretations for the silylated osmium tetroxide (OsO_4) derivatives are shown for each of these compounds: ω15,22-C_{35} methyl ketone, ω15,22-C_{36} ethyl ketone and ω16,23-C_{36} methyl ketone. The other labeled chromatographic peaks correspond to the C_{37}–C_{39} series of di-unsaturated (:2) and tri-unsaturated (:3), methyl (m) and ethyl (e) ketones that were detected in CCMP1742 as the exclusive set of alkenones prior to August, 2002 (see text for further details). Double bond positions indicated for all other di-unsaturated alkenones in each chromatogram were also determined by the same OsO_4 derivatization method. Peaks marked with an asterisk (*) correspond to three different C_{36} alkenoates commonly found in *E. huxleyi* (Brassell, 1993; Conte et al., 1998).

isothermal (15 °C), physiological stress experiments. These experiments evaluated alkenone compositional response when cells: (1) are exposed to continuous darkness for multiple days; (2) experience widely different ambient light intensities during an otherwise equivalent daily light:dark (L/D) cycle; and (3) encounter nutrient-depleted growth conditions. All three of these conditions potentially act to some extent upon cells that grow in natural surface waters and contribute to the alkenone flux preserved in the sedimentary record (e.g., Prahl et al., 2006). The results demonstrate that alkenone distributions respond to non-thermal environmental conditions, but extreme variations in such conditions seem to be required to effect significant change in the $U^{K'}_{37}$ index value.

3.4. Continuous darkness experiments with cultures

In August of 2002, two parallel continuous darkness experiments were carried out. In both cases, cells were initially grown exponentially under a 12:12 h L/D cycle until nitrate-depleted. At that point, one culture flask was covered with aluminum foil and maintained by that means in complete darkness for 5 days. Nutrient medium was added to the second flask prior to shifting it, by identical means, to the same darkness conditions. Afterwards, the aluminum foil was removed and both flasks were returned to their previous L/D cycle. Throughout each experiment, cell density and nutrients were monitored daily and cell samples were collected for alkenone analysis (see Dark Shift #1 and #2, Table 1).

In both cases, the cellular content of total C_{35}–C_{39} alkenones (Fig. 1) decreased with time under complete darkness by a factor of 2–3. Loss of C_{37} di-unsaturated and tri-unsaturated alkenones occurred disproportionately, leading to a progressive increase in $U^{K'}_{37}$ values during the dark period (Fig. 2B). Comparable compositional changes were documented in similar experiments run with CCMP1742 prior to appearance of the new alke-

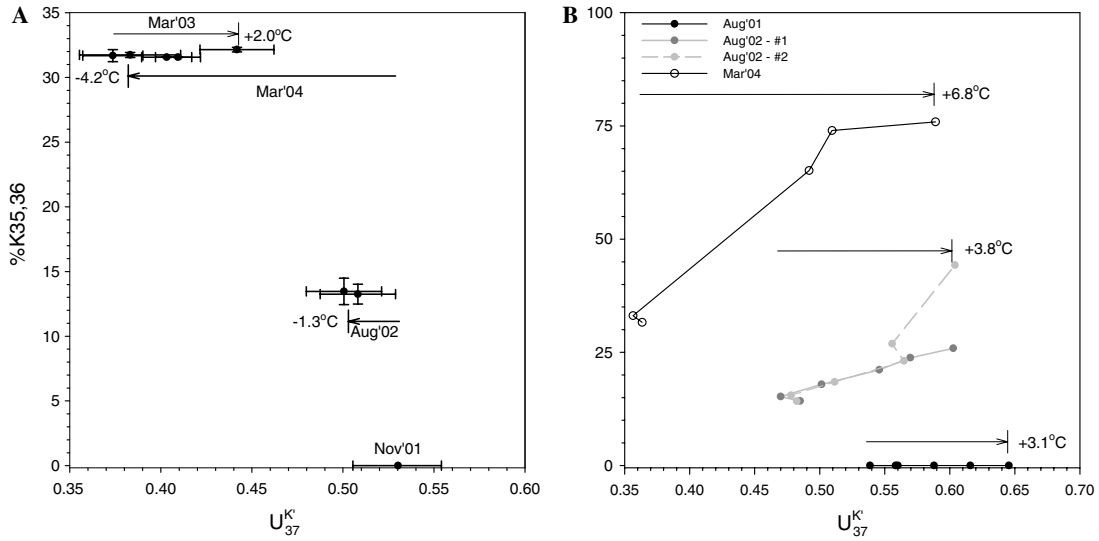

Fig. 2. Scatter plot for the percentage contribution of the new C_{35} and C_{36} alkenones to total C_{35}–C_{39} alkenones (%K35,36) versus values for the alkenone unsaturation index $U^{K'}_{37}$ measured: (A) in exponentially dividing cells from each of the seven batch culture experiments conducted in this study; and (B) in cells exposed to 5 days of complete darkness in three of these experiments. All experiments were run isothermally at 15 °C. All data shown, except those for November of 2001 (Prahl and Sparrow, unpublished results) and August of 2001, were obtained from Table 1. $U^{K'}_{37}$ values for August of 2001 were calculated from alkenone concentration data reported elsewhere (see Table 1 in Prahl et al., 2003: erratum—column labels for K37:2 and K37:3 are reversed). The dashed horizontal arrows drawn on both plots gauge the magnitude that $U^{K'}_{37}$ changed in the different experiments as a consequence of various, non-thermal physiological stresses (see text for further details). Numbers associated with each arrow indicate the extent that growth temperature would have had to increase (or decrease) in order to yield the observed non-thermal, physiological changes in $U^{K'}_{37}$. Calculations were made assuming $U^{K'}_{37}$ values would change by +0.034 units per °C of growth temperature (Prahl et al., 1988).

nones (Prahl et al., 2003). Darkness also led to a systematic change in some, but not all, aspects of the new alkenone composition. Over the exposure period, the percentage of new to total alkenones (%K35,36) increased by a factor $\geqslant 2$ (Fig. 2B), while the percentage of C_{35} to all new alkenones (%K35) declined from an initial value of ~68% to a final value of 62% (Fig. 3A). There was no clear effect of darkness on the proportion of the C_{36} methyl to ethyl alkenone (K36e/m). Upon reinstatement of the daily L/D cycle, all compositional attributes of the alkenones recovered within 2 days to values approaching those characteristic of cells analyzed prior to continuous darkness exposure (Table 1). Thus, the observed compositional changes appear to be a physiological response of living cells to darkness and not due to some other biological process(es) that potentially could be occurring in our non-axenic cultures.

About 1.5 years later in March of 2004, another darkness experiment was conducted in a similar manner to that described above. In this case, however, darkness was imposed on cells prior to the onset of nitrate depletion in the medium. The impact of darkness on alkenone compositions followed the same general pattern just described. Nonetheless, two specific differences are quite noteworthy. By the end of the darkness period (1) the positive shift in $U^{K'}_{37}$ values was approximately twice the magnitude of that observed in the experiments a year earlier and (2) the new C_{35} and C_{36} compounds accounted for 76% of the total C_{35}–C_{39} alkenone content, more than twice the initially high proportion of 32% (Fig. 2B).

3.5. Contrasting light exposure experiments

In March of 2003, four parallel, isothermal (15 °C) batch culture experiments were conducted with CCMP1742 to test the effect of light intensity on alkenone biosynthetic patterns. With the exception of one key difference, all culture flasks were set up identically. One flask was exposed to full light intensity (240 μEin m^{-2} s^{-1}), while the others were exposed to 50%, 25% and 12.5% of full light intensity. The required shading for the other three flasks was accomplished by wrapping with one, two and three layers of neutral density screen, respectively.

In each case, the average specific growth rate (μ) was assessed by monitoring cell density daily through the period of exponential growth (complete data set not tabulated). The value for μ was defined by the slope of the line resulting from Model I least squares regression analysis of the natural logarithm of cell density versus time. Values assessed in this way were greatest at the highest light intensity (0.63 ± 0.022 d^{-1} $p < 0.0001$ at 240 μEin m^{-2} s^{-1}), declined only slightly as light intensity was halved (0.59 ± 0.037 d^{-1} $p < 0.0001$) and quartered (0.58 ± 0.019 d^{-1} $p < 0.0001$), but dropped off quite significantly at the lowest light intensity (0.50 ± 0.024 d^{-1} $p < 0.0001$). Based on these results, light-saturated growth (μ_{max}) for our stock of CCMP1742 in its current physiological form appears to occur at PAR values between 30 and 60 μEin m^{-2} s^{-1}. This inference is consistent with observations reported by Muggli and Harrison (1996) for another strain of *E. huxleyi* (NEPCC732) that, like CCMP1742, was originally isolated from Station

Table 1
Summary of results from analysis of seven isothermal (15 °C) batch culture experiments run with our strain of *E. huxleyi* (CCMP1742) that is now biosynthesizing new di-unsaturated C_{35} (methyl) and C_{36} (methyl and ethyl) ketones

Experiment	Day[a]	Condition	Cell density (per mL)	Nitrate (μM)	Phosphate (μM)	ΣK_{35-39} (pg/cell)	$U^{K'}_{37}$	%K35,36	%K35	K36e/m (%)
Dark Shift #1	−3	Light/dark	2.91E+05	78.0	7.2	1.76	0.52	13	68	80
August 2002	−2	Light/dark	4.75E+05	61.4	6.0	1.52	0.47	15	68	75
	−1	Light/dark	6.81E+05	32.8	4.0	1.32	0.50	14	68	82
	0	Light/dark	9.87E+05	0.5	1.5	1.36	0.48	14	68	82
	1	Darkness	1.42E+06	0.4	0.7	0.87	0.47	15	68	78
	2	Darkness	1.35E+06	0.3	0.2	0.66	0.50	18	66	79
	3	Darkness	1.42E+06	0.2	0.1	0.58	0.55	21	65	81
	4	Darkness	1.39E+06	0.2	0.1	0.61	0.57	24	64	76
	5	Darkness	1.39E+06	0.2	0.2	0.30	0.60	26	62	75
		Light/dark	1.39E+06	0.1	0.1	0.93	0.61	19	64	79
		Light/dark	1.46E+06	0.0	0.1	1.69	0.54	18	62	80
Dark Shift #2	−3	Light/dark	3.79E+05	71.4	6.6	1.36	0.52	13	68	91
August 2002	−2	Light/dark	5.80E+05	51.8	5.1	1.61	0.51	13	68	83
	−1	Light/dark	8.36E+05	22.4	2.8	1.41	0.50	14	68	88
	0	Light/dark	1.08E+06	89.8	2.9	1.47	0.48	14	69	93
	1	Darkness	1.41E+06	81.4	2.0	0.75	0.48	15	69	88
	2	Darkness	1.50E+06	70.3	0.9	0.58	0.51	18	67	87
	3	Darkness	1.51E+06	59.9	0.2	0.40	0.56	23	65	87
	4	Darkness	1.61E+06	49.5	0.1	0.54	0.56	27	63	88
	5	Darkness	1.51E+06	36.1	0.1	0.45	0.60	44	61	84
		Light/dark	1.57E+06	12.8	0.1	2.06	0.67	21	64	90
		Light/dark	1.45E+06	0.2	0.1	1.16	0.55	19	64	89
240 μEin m^{-2} s^{-1}	−5	Light/dark	4.78E+05	58.6	2.6	0.68	0.40	31	68	96
March 2003	−4	Light/dark	6.87E+05	33.8	0.9	0.99	0.38	32	67	96
	−3.75	Light/dark	8.65E+05	25.0	0.5	1.08	0.35	32	67	84
	−3.5	Light/dark	8.55E+05	17.4	0.2	1.17	0.37	32	68	87
	−3.25	Light/dark	9.62E+05	12.7	0.1	1.03	0.37	32	67	84
	−3	Light/dark	1.02E+06	7.8	0.2	1.22	0.37	32	68	95
	1	Light/dark, nutrient depletion	2.72E+06	0.3	0.1	2.08	0.33	30	58	76
	2	Light/dark, nutrient depletion	2.97E+06	0.2	0.1	2.59	0.33	30	56	71
120 μEin m^{-2} s^{-1}	−5		3.89E+05	62.9	4.0	0.80	0.41	32	66	83
March 2003	−4		4.43E+05	43.1	2.6	1.33	0.39	32	68	83
	1	Light/dark, nutrient depletion	2.89E+06	0.3	0.1	1.84	0.35	31	59	84
	2	Light/dark, nutrient depletion	3.00E+06	0.4	0.1	2.33	0.34	30	57	80
60 μEin m^{-2} s^{-1}	−5	light/dark	3.37E+05	64.1	4.1	1.04	0.42	32	67	82
March 2003	−4	Light/dark	4.83E+05	45.9	2.8	1.03	0.40	32	68	87
	1	Light/dark, nutrient depletion	2.91E+06	0.3	0.1	1.98	0.38	31	59	89
	2	Light/dark, nutrient depletion	2.97E+06	0.4	0.1	2.14	0.36	30	58	86
30 μEin m^{-2} s^{-1}	−5	Light/dark	1.53E+05	74.7	4.9	0.89	0.47	32	68	92
March 2003	−4	Light/dark	2.06E+05	66.2	4.3	1.27	0.45	32	68	97
	−3.75	Light/dark	2.49E+05	63.2	4.2	1.33	0.41	32	68	87
	−3.5	Light/dark	3.39E+05	60.0	3.9	1.13	0.46	32	67	93
	−3.25	Light/dark	4.16E+05	57.6	3.6	0.98	0.44	32	67	93
	−3	Light/dark	5.12E+05	53.7	3.4	0.84	0.43	32	69	101
	1	Light/dark, nutrient depletion	2.54E+06	0.4	0.1	1.53	0.38	31	62	90
	2	Light/dark, nutrient depletion	2.06E+06	0.3	0.1	2.73	0.39	31	60	84
Dark Shift #3	−1	Light/dark	2.43E+05	63.6	2.7	0.42	0.40	32	65	76
March 2004	0	Light/dark	4.98E+05	50.5	1.6	0.88	0.36	32	66	83
	1	Darkness	3.88E+05	48.5	1.1	0.82	0.36	33	66	82
	3	Darkness	3.84E+05	45.4	1.1	0.21	0.49	65	64	84
	4	Darkness	3.36E+05	40.5	1.1	0.15	0.51	74	63	79
	5	Darkness	3.80E+05	37.4	0.9	0.13	0.59	76	62	74
		Light/dark	5.50E+05	26.3	0.4	0.80	0.47	37	64	79
		Light/dark	6.82E+05	6.3	0.2	1.48	0.37	33	65	80

[a] Number of days before (negative values) or after (positive values) the stress of either darkness or nutrient depletion occurred; shaded data in each experiment highlights the period of stress.

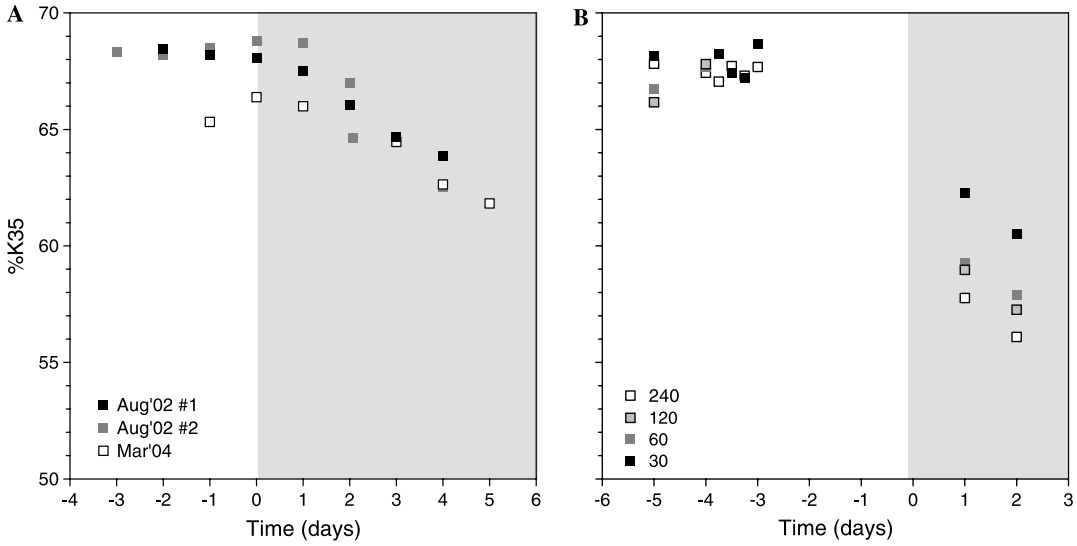

Fig. 3. Scatter plot showing relationship between the percentage contribution of C_{35} to total new C_{35} and C_{36} alkenones (%K35) and $U^{K'}_{37}$ measured in our stock of CCMP1742 cells stressed by exposure in: (A) to 5 days of continuous darkness; and (B) to both increasing light intensity (30, 60, 120, 240 μEin m^{-2} s^{-1}) and nutrient depletion. The shaded area in plots (A) and (B) indicate the experimental periods of continuous darkness and nutrient depletion, respectively.

PAPA in the subarctic Pacific Ocean. The value of μ_{max} determined for CCMP1742 in our present set of experiments (~0.6 d^{-1}) falls at the lowest end of the range observed in *E. huxleyi* strains isolated from widely different oceanographic regions (0.6–2.8 d^{-1}; Paasche, 2002).

During the nutrient-replete period of exponential growth, cell samples were collected for alkenone analysis on three consecutive days in the high and low light experiments and two consecutive days in the two mid-light cases (Table 1). In the high and low light experiments, cells were also collected every 6 h for a 24 h period after the second daily sample was taken. Results from all of these sample analyses indicate that the total alkenone content (ΣK_{35-39}) of cells, the fractional contribution of new to total alkenones (%K35,36) and the fractional contribution of C_{35} to total new alkenones (%K35) have no clear dependence on light intensity. Values of ΣK_{35-39} and, in particular, of the proportions %K35,36 and %K35, which are the easiest properties to analyze precisely, are remarkably uniform in the complete sample set, averaging 1.05 ± 0.19 pg/cell, $32 \pm 0.4\%$ and $68 \pm 0.6\%$, respectively. $U^{K'}_{37}$ was the only compositional property that displayed any evidence for dependence on light intensity. Results show a progressive increase of +0.07 $U^{K'}_{37}$ units in exponentially growing cells as light intensity was decreased in three geometric steps from 240 to 30 μEin m^{-2} s^{-1}. This magnitude of $U^{K'}_{37}$ response to varied light intensity is equivalent to what would be expected if growth temperature in this isothermal experiment had been increased by +2.0 °C (Fig. 2A). A similar response of $U^{K'}_{37}$ to decreasing light intensity has previously been documented for alkenones biosynthesized by the haptophyte *Isochrysis galbana* when cultured at a comparable isothermal growth temperature (16 °C; Versteegh et al., 2001).

3.6. Nutrient-depletion experiments

Cells in each of the four culture flasks from the light exposure experiment were allowed to continue growing until the medium was depleted of nutrients. At that point, cells stopped dividing and entered a stationary growth phase. On two consecutive days, cell samples were taken from each culture flask for alkenone analysis. Regardless of the light level, ΣK_{35-39} content increased in the stationary growth phase cells by a factor of ~2 relative to nutrient-replete, exponentially dividing cells. Also, $U^{K'}_{37}$ values decreased in each case by nearly the same amount, i.e., ~0.05 units. Comparable trends for alkenone content (ΣK_{35-39}) and unsaturation pattern ($U^{K'}_{37}$) were evident when nutrient-depletion experiments were conducted with the same stock of CCMP1742 prior to the appearance of new alkenones in cells (Prahl et al., 2003).

Nutrient depletion caused notable change in some, but not all, of the properties defined to describe the new alkenone composition. %K35,36 values decreased slightly, indicating that the accumulation of total alkenones in stationary growth phase cells occurs with some degree of discrimination against the new compounds. The decrease in %K35 values was far more pronounced, indicating that alkenone accumulation in the stationary growth phase cells favored C_{36} over C_{35} compounds. Furthermore, the effect on %K35 was greater in cells exposed to higher light levels (Fig. 3B). Given the data set available, the response of K36e/m to nutrient stress cannot be judged so confidently, however. At the highest light intensity, measured values for this property were markedly lower in stationary phase cells. But, at the other light exposure levels, K36e/m values measured in exponentially dividing cells and stationary growth phase cells showed no discernable difference.

3.7. Unusual alkenone signatures in natural waters and sediments

C_{37}–C_{39} alkenones occur almost ubiquitously in surface waters and underlying sediments throughout the ocean (Brassell, 1993). Alkenone signatures detected in Modern open ocean samples are generally consistent with the dominant contributing source being *E. huxleyi* and perhaps its close relative *Gephyrocapsa oceanica* in equatorial regions (Müller et al., 1998). In some lacustrine and inland sea environments, the alkenone signature imprinted on samples can deviate significantly from that expected for *E. huxleyi* (Schulz et al., 2001; Xu et al., 2001; Zink et al., 2001; Chu et al., 2005). These compositional deviations provide diagnostic signs that sources other than *E. huxleyi* likely account for the biomarker signal detected in these settings.

Alkenone compositions containing unusual C_{40} compounds as minor constituents have been observed in a variety of Modern lacustrine and hypersaline settings. Since *E. huxleyi* is not reported to biosynthesize such compounds, other alkenone-producing haptophytes (Brassell, 1993) have been ascribed as the contributing source. In the case of the English lakes studied by Cranwell (1985), this inference seems unquestionable since *E. huxleyi* is physiologically incapable (Paasche, 2002) of living in the freshwater conditions of those lakes. However, Ace Lake in Antarctica and Lake Van in Turkey, other lacustrine settings where alkenones have also been observed (Volkman et al., 1988; Thiel et al., 1997), are both quite saline. Recent genetic analysis of DNA preserved in Ace Lake sediments now provide convincing additional evidence that the anomalous alkenone signature in that lake derives from close relatives of the haptophyte *I. galbana* and not *E. huxleyi* (Coolen et al., 2004). In hypersaline coastal microbial mats, the observed alkenone signatures are characterized by a lack of even-chain methyl and odd-chain ethyl ketones (Lopez and Grimalt, 2005; Lopez et al., 2005; Rontani and Volkman, 2005), and bear a close similarity with that now recognized in *Chrysotila lamellosa* (Marlowe et al., 1984; Rontani et al., 2004).

Two unusual di-unsaturated C_{35} methyl and C_{36} ethyl ketones have been detected as minor constituents of alkenone compositions in SPM from the Ligurian Sea in the NW Mediterranean (Rontani et al., 2001). Although double bond positions were not determined in that prior work, one might now assign them as ω15,22 di-unsaturated C_{35} methyl ketone (K36:2m) and C_{36} ethyl ketone (K36:2e), the compounds being produced in culture by our specimen of CCMP1742 (Fig. 1). And, on this basis, one might assign *E. huxleyi*, a well-recognized component of the overall phytoplankton community in surface waters of the Ligurian Sea (Ternois et al., 1997), as a potential source of these compounds. However, three conspicuous compositional differences would challenge such an inference. First, K36:2e is the dominant component in the field sample while that in our culture is K35:2m. Second, CCMP1742 biosynthesizes a third compound, ω16,23-K36:2m (Fig. 1), that was not detected in the field sample (Rontani et al., 2001). And third, the gas chromatographic retention time for K35:2m and K36:2e identified in the natural field and laboratory culture samples are not identical (Fig. 4). Thus, these compounds must be isomers and hence indicative of a variation in the biosynthetic pathway which is most likely associated with a different organism. Although these facts alone are not unequivocal proof, they do provide circumstantial evidence that some haptophyte source in addition to *E. huxleyi* contributes to the alkenone signature in surface waters of the Ligurian Sea.

3.8. Unusual alkenone signatures in contemporary Black Sea sediments

Emiliania huxleyi is quite productive today in surface waters of the Black Sea (Eker et al., 1999). The calcium carbonate ($CaCO_3$) content of sediments now depositing in this inland sea is comprised primarily of coccoliths almost exclusively derived from this specific coccolithophorid (Bukry, 1974). This characteristic of the $CaCO_3$ content is a feature of sediments that have been accumulating in the Black Sea over the past three to four millennia as a deposit known as Unit I (Arthur and Dean, 1998). In addition to the coccolith record, evidence for significant *E. huxleyi* contribution is clearly imprinted in the organic matter fraction of Unit I sediments by the abundant presence of this organism's characteristic C_{37}–C_{39} alkenone fingerprint (de Leeuw et al., 1980; Xu et al., 2001).

The top chromatogram in Fig. 5 illustrates the alkenone plus alkenoate signature preserved in the Unit I deposit from the Black Sea that we analyzed and the dominance of C_{37}–C_{39} alkenones derived from *E. huxleyi*. Unusual di-unsaturated C_{35} methyl and C_{36} ethyl ketones as well as a di-unsaturated C_{34} alkenoate are also observed as minor, but clearly detectable, components of this signature. The former alkenones have identical gas chromatographic retention times with those detected in SPM from the Ligurian Sea (Fig. 4), suggesting that they are structurally the same. As revealed by our GC–MS analysis of OsO_4 derivatives, the double bonds are located at positions (ω15,20) in the carbon chain quite different from that of the otherwise equivalent new compounds now found in CCMP1742 (Fig. 1) and commonly considered normal (ω15,22) for alkenone (and alkenoate) biosynthesis by *E. huxleyi* (Brassell, 1993 and references therein).

Xu et al. (2001) first documented the occurrence of K36:2e with the unusual ω15,20 double bond pattern in Black Sea sediments. Our work on Unit I sediments from a second coring site located ~210 km to the east supports their finding and formally establishes the position of double bonds in the carbon chain of K35:2m, the other unusual alkenone they detected but did not structurally characterize in their reported work. As previously suggested, it seems likely that

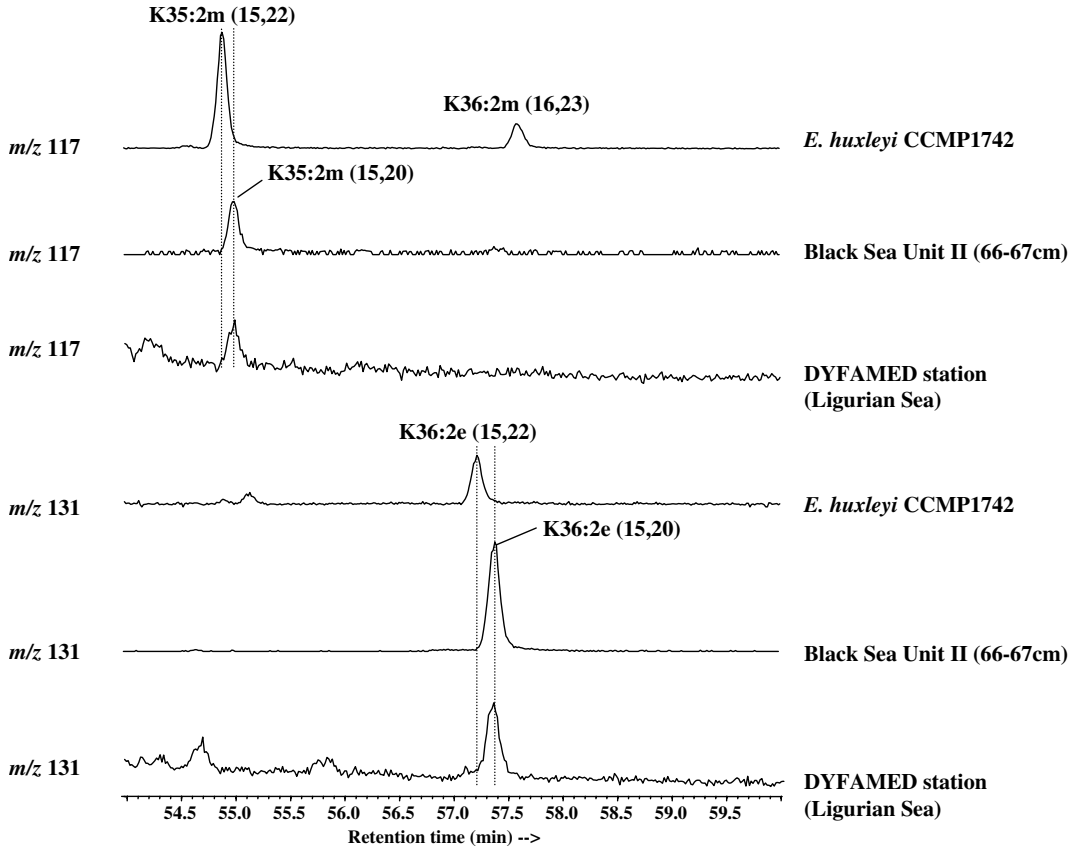

Fig. 4. Comparison of mass fragmentograms for di-unsaturated C_{35} and C_{36} ketone (analyzed as silylated alkenol derivatives) composition measured in suspended particulate materials (SPM) from surface waters in the Ligurian Sea (DYFAMED station; Rontani et al., 2001) with that measured in cells of *E. huxleyi* (CCMP1742) grown in batch culture under laboratory controlled conditions and in a sediment interval (66–67 cm) from Unit II of Black Sea gravity core (BS4-14-2GC). Alkenol derivatives of methyl and ethyl ketones were detected using *m/z* 117 and *m/z* 131 selective ion monitoring, respectively. Alkenones were reduced in diethyl ether–methanol (2:1, v/v) (5 mL) with excess $NaBH_4$ (10 mg/mg of extract). The resulting alkenols were subsequently extracted according to a previously described procedure (Rontani et al., 2001) and silylated before GC–MS analyses. The GC–MS conditions employed are described in Section 2.

two different haptophyte sources have contributed to the alkenone signature preserved in Unit I sediments. Furthermore, the presumed second alga appears to be productive today not only in the Black Sea but also in the Ligurian Sea. Further organic geochemical study facilitated by use of genetic techniques (e.g., Coolen et al., 2004) are needed to prove this inference and may well show the presence of this additional alkenone-producer throughout the Mediterranean. The broad geographic distribution already apparent from our limited data implies that *E. huxleyi* and this presumed second source are both able to tolerate growth under the wide range of surface water salinity (~20 to >35) that characterizes these environments.

3.9. Unusual alkenone signatures in the early Holocene Black Sea

An abrupt stratigraphic change in sediment lithology depicts succession of the Black Sea during the early Holocene from a lake to an inland sea mode of operation (Arthur and Dean, 1998 and references therein). However, the lithological change from the lacustrine deposit (Unit III) to the marine deposit observed today (Unit I) did not occur as a smooth, one-step transition. Rather, sedimentation under salinity-stratified inland sea conditions led first to formation of a laminated, very organic-rich (⩽20% by weight, or 'sapropelic') deposit containing 5–15% $CaCO_3$ content (Unit II) and subsequently to the laminated marl observed today (Unit I).

Although *E. huxleyi* is the dominant $CaCO_3$ contributor to Unit I, the early Holocene assemblage of coccolithophorids contributing to the $CaCO_3$ content of Unit II is much more diverse (Bukry, 1974). The conspicuous change in the coccolith assemblage between Unit II and I is thought to demark the time in the Black Sea's evolution when average surface water salinity exceeded the minimum calcification threshold for a low salinity-tolerant coccolithophorid like *E. huxleyi*. The implication is that *E. huxleyi*, presumably seeded by inflow of Mediterranean waters, first successfully 'invaded' the Black Sea at that time (e.g., see Arthur and Dean, 1998).

As in Unit I, alkenones are abundantly present at most depths in the Unit II deposit (Xu et al., 2001). Thus,

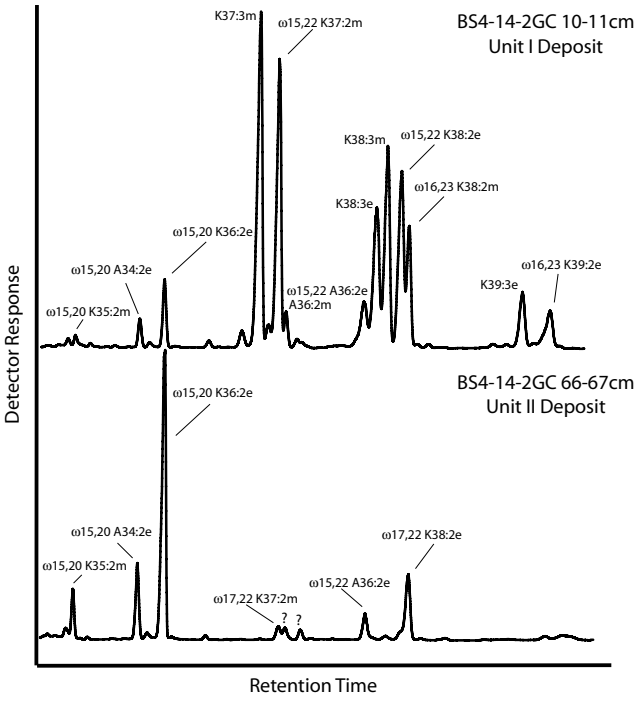

Fig. 5. Comparison of alkenone and alkenoate compositions observed in two depth intervals from a Black Sea core (BS4-14-2GC) representing the Holocene Unit I (10–11 cm) and Unit II (66–67 cm) deposit (Arthur and Dean, 1998), respectively. Alkenones (K) and alkenoates (A) are identified by the codes: K##:# or A##:#, where ##:# represents the carbon-chain length:number of double bonds while m and e represents methyl ketone and ethyl ketone or ester, respectively. The position of double bonds in the carbon chain are indicated in ω-notation (i.e., relative to the non-functionalized end of the molecule) in all cases where we actually made OsO_4 derivatives of di-unsaturated compounds for GC–MS analysis.

alkenone-producing haptophytes (Green and Leadbeater, 1994) of some type were contributing to primary productivity in the Black Sea in the earliest stages of its evolution from a lake into an ocean-connected inland sea. However, the alkenone fingerprint preserved in Unit II deviates significantly from that characteristic of *E. huxleyi*. Although the composition documented by Xu et al. (2001) bears some semblance, the typically conspicuous C_{37} and to a lesser extent C_{39} components in *E. huxleyi* are virtually absent in the Unit II interval examined in our study (bottom chromatogram, Fig. 5). The dominant components are the ω15,20 di-unsaturated C_{35} methyl and C_{36} ethyl ketones and C_{34} ethyl alkenoate that were observed as minor components in the Unit I deposit (top chromatogram, Fig. 5). These compounds are accompanied by ω17,22 di-unsaturated C_{37} methyl and C_{38} ethyl ketones and ω15,22 C_{36} ethyl alkenoate. All of the latter compounds are quite likely also present in the fingerprint for Unit I sediments but their detection is obscured by coelution with corresponding, more dominant components typical of *E. huxleyi*. The A36:2e alkenoate is the only haptophyte-derived biomarker detected in the Unit II deposit characterized by double bonds located in carbon-chain positions expected for *E. huxleyi*.

3.10. Biosynthetic and paleoceanographic generalizations

The presence of C_{35} and C_{36} alkenones and a C_{34} alkenoate in Black Sea sediments, although a most unusual finding, does not in itself discount contribution from *E. huxleyi* given the serendipitous appearance of compounds with such short carbon-chain length recently in our culture of CCMP1742. However, occurrence of double bonds in positions uncharacteristic of those expected for *E. huxleyi* does now argue more persuasively for the source of these unusual compounds in Unit I and Unit II sediments from the Black Sea being some other haptophyte species.

Our culture work in the present study has produced some new insight to the pathway of alkenone and alkenoate biosynthesis. Results presented in Fig. 1 show that double bonds do not occur at the same fixed distance from the alkyl end of the molecule as limited literature on this topic would currently suggest (see Brassell, 1993 and references therein). Compounds with ω15,22 and ω16,23 double bonds were detected in CCMP1742 (Fig. 1). Re-investigation of the double bond positions of classical C_{37}–C_{40} alkenones showed that unsaturations are located quite notably at the same fixed distance in the carbon chain from the ketone functionality (Rontani et al., 2006b). These very surprising results may explain the recent detection of C_{39} and C_{40} alkenones with anomalous ω16,23 and ω17,24 double bond positions in hypersaline sediments (Lopez and Grimalt, 2005; Lopez et al., 2005). These observations could be accounted for if the carbon chain for C_{37}–C_{40} alkenones were first synthesized and the double bonds then set by desaturases operating on the molecule before it separated from the enzyme in the last elongation–decarboxylation step of biosynthesis (Rontani et al., 2006b).

Interestingly, the same geometric relationship does not hold true for the three new alkenones (K35:2m, K36:2e and K36:2m) now being synthesized by CCMP1742. Double bonds in the latter compounds are located at ω15,22 and ω16,23, respectively (Fig. 1), positions which are consistent with shortening of the carbon chain in alkenone precursors having preset unsaturation patterns. In contrast, double bonds are located at ω15,20 and ω17,22 positions in shorter (K35:2m, K36:2e) and longer (K37:2m, K38:2e) chain homologues in the Unit II deposit of the Black Sea, respectively. These findings suggest the chains are all first synthesized by their yet unknown source organism and then desaturated before the molecules separate from the enzyme responsible for elongation–decarboxylation.

The haptophyte source of the unusual alkenone/alkenoate signature, if the same in all cases, appears capable of living over the same range of salinity as *E. huxleyi* judging from detection of its biomarker signature in SPM from surface waters in the Ligurian Sea (Fig. 4 and Rontani et al., 2001) and in Unit I sediments from the Black Sea (top chromatogram, Fig. 5). If the Unit II sediments were indeed deposited under low salinity conditions as currently

believed, then this organism is also capable of living at a much lower salinity. Further organic geochemical study most likely facilitated with new genetic tools (e.g., Coolen et al., 2004) will be required to explore this paleoceanographically intriguing issue further.

4. Conclusions

Our batch culture experiments with a paleoceanographic benchmark strain of *E. huxleyi* (CCMP1742) has shown the alkenone and alkenoate composition of this organism is subject to significant change not only as a consequence of variable growth temperature, but also in response to other environmentally relevant non-thermal physiological growth factors including nutrient and light availability. The mysterious appearance of entirely new alkenones of unusually short-chain length in our stock of CCMP1742 highlights the fact that much remains to be learned about the physiology of this organism and growth factors controlling biosynthesis of these novel biomarkers. $U^{K'}_{37}$ analysis has clearly proven invaluable for purposes of paleoceanographic temperature reconstruction and the index is overall surprisingly robust. However, it is now clearly recognized that non-thermal physiological impacts on this index are possible under specific conditions that can be found in natural waters and sedimentary settings (e.g., low nutrients, variable light intensity, prolonged darkness). Although there is yet no identified foolproof way to recognize when such compromise has occurred in any particular case, detailed analysis of the overall biomarker signature preserved in sediments can provide some quality assurance and should be done whenever possible. In our view, it is not sufficient to just measure the abundance of C_{37} components without considering whether the total distribution is consistent with an *E. huxleyi* source. In cases where additional sources seem likely then determination of double bond positions can provide valuable insights into their possible identity. Alkenone distributions have the potential to provide even more information than just an estimate of paleotemperature.

Acknowledgments

We are most grateful to Joe Jennings (Oregon State University) for performing all nutrient analyses, the U.S. National Science Foundation-sponsored (OCE-0351393) Core Repository at OSU for supply of Black Sea sediment samples and the U.S. NSF (OCE-9986306 and 0350409—FGP), CNRS-INSU (J.F.R.) and CSIRO (J.K.V.) for funds that supported this research. Thanks are due to Drs. J.-C. Marty and J.-C. Miquel for the sampling and initial treatment of the DYFAMED particulate matter samples used in this work. Comments from three reviewers and the Associate Editor are gratefully acknowledged.

Associate editor: David W. Lea

References

Arthur, M.A., Dean, W.E., 1998. Organic-matter production and preservation and evolution of anoxia in the Holocene Black Sea. *Paleoceanography* **13**, 395–411.

Brassell, S.C., 1993. Applications of biomarkers for delineating marine paleoclimatic fluctuations during the Pleistocene. In: Engel, M.H., Macko, S.A. (Eds.), *Organic Geochemistry: Principles and Applications*. Plenum Press, New York, pp. 699–738.

Brassell, S.C., Eglinton, G., Marlowe, I.T., Pflaumann, U., Sarnthein, M., 1986. Molecular stratigraphy: a new tool for climatic assessment. *Nature* **320**, 129–133.

Bukry, D., 1974. Coccoliths as paleosalinity indicators—evidence from Black Sea. In: Degens, E.T., Ross, D.A. (Eds.), *The Black Sea—Geology, Chemistry, and Biology*. The American Association of Petroleum Geologists, Tulsa, Oklahoma, pp. 353–363.

Chu, G., Sun, Q., Li, S., Zheng, M., Jia, M., Lu, C., Liu, J., Liu, T., 2005. Long-chain alkenone distributions and temperature dependence in lacustrine surface sediments from China. *Geochim. Cosmochim. Acta* **69**, 4985–5003.

Conte, M.H., Eglinton, G., Madureira, L.A.S., 1995. Origin and fate of organic biomarker compounds in the water column and sediments of the eastern North Atlantic. *Philos. Trans. Roy. Soc. Lond. B* **348**, 169–178.

Conte, M.H., Thompson, A., Lesley, D., Harris, R., 1998. Genetic and physiological influences on the alkenone/alkenoate versus growth temperature relationship in *Emiliania huxleyi* and *Gephyrocapsa oceanica*. *Geochim. Cosmochim. Acta* **62**, 51–68.

Coolen, M.J.L., Muyzer, G., Rijpstra, W.I.C., Schouten, S., Volkman, J.K., Sinninghe Damsté, J.S., 2004. Combined DNA and lipid analyses of sediments reveal changes in Holocene haptophyte and diatom populations in an Antarctic lake. *Earth Planet. Sci. Lett.* **223**, 225–239.

Cranwell, P.A., 1985. Long-chain unsaturated ketones in recent lacustrine sediments. *Geochim. Cosmochim. Acta* **49**, 1545–1552.

de Leeuw, J.W., van der Meer, J.W., Rijpstra, W.I.C., Schenck, P.A., 1980. On the occurrence and structural identification of long chain ketones and hydrocarbons in sediments. In: Douglas, A.G., Maxwell, J.R. (Eds.), *Advances in Organic Geochemistry 1979*. Pergamon Press, New York, pp. 211–217.

Eglinton, T.I., Conte, M.H., Eglinton, G., Hayes, J.M., 2001. Proceedings of a workshop on alkenone-based paleoceanographic indicators. *Geochem., Geophys. Geosyst.* **2**, 2000GC000122.

Eker, E., Georgieva, L., Senichkina, L., Kideys, A.E., 1999. Phytoplankton distributions in the western and eastern Black Sea in spring and autumn 1995. *J. Mar. Sci.* **56** (Suppl.), 15–22.

Epstein, B.L., d'Hondt, S., Quinn, J.G., Zhang, J., Hargraves, P.E., 1998. An effect of dissolved nutrient concentrations on alkenone-based temperature estimates. *Paleoceanography* **13**, 122–126.

Green, J.C., Leadbeater, B.S.C., 1994. *The Haptophyte Algae*. Clarendon Press, Oxford.

Lopez, J.F., Grimalt, J.O., 2005. Phenyl- and cyclopentylimino derivatization for double bond location in unsaturated C_{37}–C_{40} alkenones by GC–MS. *J. Am. Soc. Mass Spectrom.* **15**, 1161–1172.

Lopez, J.F., Garcia de Oteyza, T., Teixidor, P., Grimalt, J.O., 2005. Long chain alkenones in hypersaline and marine coastal microbial mats. *Org. Geochem.* **36**, 861–872.

Marlowe, I.T., Green, J.C., Neal, A.C., Brassell, S.C., Eglinton, G., Course, P.A., 1984. Long chain (n-C_{37}–C_{39}) alkenones in the Prymnesiophyceae. Distribution of alkenones and other lipids and their taxonomic significance. *Br. Phycol. J.* **19**, 203–216.

Muggli, D.L., Harrison, P.J., 1996. Effects of nitrogen source on the physiology and metal nutrition of *Emiliania huxleyi* grown under different iron and light conditions. *Mar. Ecol. Prog. Ser.* **130**, 255–267.

Müller, P.J., Kirst, G., Ruhland, G., von Storch, I., Rosell-Méle, A., 1998. Calibration of the alkenone paleotemperature index $U^{k'}_{37}$ based on core-tops from the eastern South Atlantic and the global ocean (60°N–60°S). *Geochim. Cosmochim. Acta* **62**, 1757–1772.

Paasche, E., 2002. A review of the coccolithophorid *Emiliania huxleyi* (Prymnesiophyceae), with particular reference to growth, coccolith formation and calcification—photosynthesis interaction. *Phycologia* **40**, 503–529.

Prahl, F.G., Mix, A.C., Sparrow, M.A., 2006. Alkenone paleothermometry: lessons from marine sediment records off western South America. *Geochim. Cosmochim. Acta* **70**, 101–117.

Prahl, F.G., Muehlhausen, L.A., Lyle, M., 1989. An organic geochemical assessment of oceanographic conditions at MANOP Site C over the past 26,000 years. *Paleoceanography* **4**, 495–510.

Prahl, F.G., Muehlhausen, L.A., Zahnle, D.L., 1988. Further evaluation of long-chain alkenones as indicators of paleoceanographic conditions. *Geochim. Cosmochim. Acta* **52**, 2303–2310.

Prahl, F.G., Popp, B.N., Karl, D.M., Sparrow, M.A., 2005. Ecology and biogeochemistry of alkenone production at Station ALOHA. *Deep-Sea Res. I* **52**, 699–719.

Prahl, F.G., Wolfe, G.V., Sparrow, M.A., 2003. Physiological impacts on alkenone paleothermometry. *Paleoceanography* **18**, 1025. doi:10.1029/2002PA000803.

Rechka, J.A., Maxwell, J.R., 1988. Characterization of alkenone temperature indicators in sediments and organisms. *Org. Geochem.* **13**, 727–734.

Rontani, J.-F., Beker, B., Volkman, J.K., 2004. Long-chain alkenones and related compounds in the benthic haptophyte *Chrysotila lamellosa* Anand HAP 17. *Phytochemistry* **65**, 117–126.

Rontani, J.-F., Marchand, D., Volkman, J.K., 2001. $NaBH_4$ reduction of alkenones to the corresponding alkenols: a useful tool for their characterization in natural samples. *Org. Geochem.* **32**, 1329–1341.

Rontani, J.-F., Marty, J.-C., Miquel, J.C., Volkman, J.K., 2006a. Free radical oxidation (autoxidation) of alkenones and other microalgal lipids in seawater. *Org. Geochem.* **37**, 354–368.

Rontani, J.-F., Prahl, F.G., Volkman, J.K., 2006b. Re-examination of the double bond positions of alkenones and derivatives: biosynthetic implications. *J. Phycol.*, in press.

Rontani, J.-F., Volkman, J.K., 2005. Lipid characterization of coastal hypersaline cyanobacterial mats from the Camargue (France). *Org. Geochem.* **36**, 251–272.

Schulz, H.-M., Schoner, A., Emeis, K.-C., 2001. Long-chain alkenone patterns in the Baltic sea—an ocean–freshwater transition. *Geochim. Cosmochim. Acta* **64**, 469–477.

Strickland, J.D.H., Parsons, T.R., 1972. *A Practical Handbook of Seawater Analysis*. Fisheries Research Board of Canada, Ottawa, Canada.

Ternois, Y., Sicre, M.-A., Boireau, A., Conte, M.H., Eglinton, G., 1997. Evaluation of long-chain alkenones as paleo-temperature indicators in the Mediterranean Sea. *Deep-Sea Res. I* **44**, 271–286.

Thiel, V., Jenisch, A., Landmann, G., Reimer, A., Michaelis, W., 1997. Unusual distributions of long-chain alkenones and tetrahymanol from the highly alkaline Lake Van, Turkey. *Geochim. Cosmochim. Acta* **61**, 2053–2064.

Versteegh, G.J.M., Riegman, R., de Leeuw, J.W., Jansen, J.H.F., 2001. $U^{K'}_{37}$ values for *Isochrysis galbana* as a function of culture temperature, light intensity and nutrient concentrations. *Org. Geochem.* **32**, 785–794.

Volkman, J.K., Barrett, S.M., Blackburn, S.I., Sikes, E.L., 1995. Alkenones in *Gephyrocapsa oceanica*: implications for studies of paleoclimate. *Geochim. Cosmochim. Acta* **59**, 513–520.

Volkman, J.K., Burton, H.R., Everitt, D.A., Allen, D.I., 1988. Pigment and lipid compositions of algal and bacterial communities in Ace Lake, Vestfold Hills, Antarctica. *Hydrobiologia* **165**, 41–57.

Xu, L., Reddy, C.M., Farrington, J.W., Frysinger, G.S., Gaines, R.B., Johnson, C.G., Nelson, R.K., Eglinton, T.I., 2001. Identification of a novel alkenone in Black Sea sediments. *Org. Geochem.* **32**, 633–645.

Zink, K.-G., Leythaeuser, D., Melkonian, M., Schwark, L., 2001. Temperature dependency of long-chain alkenone distributions in Recent and fossil limnic sediments and in lake waters. *Geochim. Cosmochim. Acta* **65**, 253–265.